

Filament bunch formation upon femtosecond laser pulse propagation through the turbulent atmosphere.

Part 2. Statistical characteristics

S.A. Shlenov and V.P. Kandidov

International Educational-Scientific Center at the M.V. Lomonosov Moscow State University, Moscow

Received May 17, 2004

Multifilamentation of a high-power femtosecond laser pulse is investigated numerically based on the model of phase screens emulating the wide-band atmospheric turbulence. As an example, a single phase screen is used to analyze the stochastic process of a successive filamentation and statistical characteristics of these filaments. It is shown that the probability of observing large number of filaments increases with distance. It has been established by use of the Monte Carlo technique that statistical characteristics of the filament bunch are strongly dependent on the structure constant C_n^2 , while the dependence on the inner scale of turbulence l_0 is rather weak.

Based on the model of phase screens developed in Ref. 1, this paper analyzes formation of spatiotemporal traces of hot spots in the laser beam cross section, which form the filament bunch. The Monte Carlo technique is used to study the statistical characteristics of the filament bunch upon scattering of the pulse on the phase screen and its propagation in the turbulent atmosphere.

Stochastic formation of filaments

It is convenient to start analyzing the formation of multiple filaments in the turbulent atmosphere from the example of individual realizations of the propagation of a high-power beam ($P_0 \gg P_{cr}$) behind a phase screen. For the screen used, the value of phase fluctuations corresponds to the propagation along a 10-m long path in the medium with the structure constant $C_n^2 = 1.5 \cdot 10^{-14} \text{ cm}^{-2/3}$, the outer scale of turbulence $L_0 = 1 \text{ m}$, and the inner scale of turbulence $l_0 = 1 \text{ mm}$. We consider pulses with the parameters characteristic of field experiments²⁻⁵: duration of 100 fs, wavelength $\lambda = 800 \text{ nm}$, peak power P_0 of $2 \cdot 10^{11} \text{ W}$, which is roughly 30 times higher than the critical power of self-focusing in the air. The beam radius a_0 at the e^{-1} level is 0.92 cm.

The comparative analysis of the spatial scales of the light field and atmospheric turbulence is shown in Fig. 1. A dark circle of the radius a_0 , characterizing the size of the laser beam, is superimposed on the phase screen. The inner scale of turbulence l_0 is shown as a bar at the lower right. The characteristic size of the filament formed can be shown by a small dot on this scale. The outer scale of turbulence L_0 almost 50 times exceeds the linear size of the window shown in Fig. 1.

Dark spots on the phase screen are the places of local focusing of the radiation in the pulsed beam cross section. The white circles show those focusing areas, which contain the power on the order of the critical

one. The radius of the area located closer to the cross section center is about 1.6 mm. The root-mean-square phase fluctuations on this scale, as follows from the analysis of the structure function,¹ amount to about 0.1 rad. The radius of the circle encompassing the critical power at the pulse periphery, where the intensity is lower than in the axial zone, increases to 3 mm. It should be expected that just these parts of the pulse cross section can be the places of filamentation. The focusing area closest to the center has the smallest scale, and just here, we can expect the appearance of the first filament.

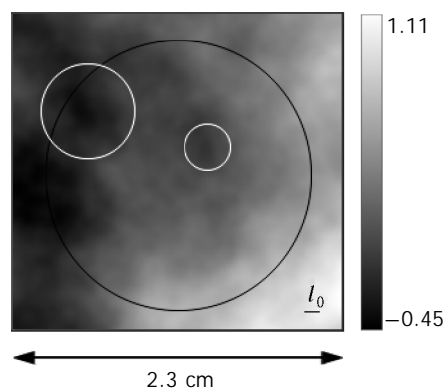


Fig. 1. Gray-scale pattern of phase fluctuations on the fragment of the 2.3x2.3 cm phase screen with the characteristic spatial scales of the light field and turbulence: laser beam (dark circle), areas containing critical self-focusing power (white circles); the inner scale l_0 is shown by the bar at the lower right.

The formation of hot spots during multifilamentation of the laser pulse was studied through numerical solution of the stochastic equation for the slowly varying amplitude of the light field.¹

The detailed calculation of the pattern of beam propagation shows that, as the pulse propagates, the positive intensity fluctuation arising at the place of the central "focusing lens" (Fig. 2, bright white spot

to the upper right from the center) forms, at the distance z_f , the nonlinear focus with the explosive increase of the intensity and, consequently, a filament is formed here.



Fig. 2. Intensity distribution in the pulse cross section at the distance $z = 21$ m behind the phase screen. The bright white spot near the beam center indicates the formation of the first filament.

Although the appearance of the second and following filaments at some places depends on the phase fluctuations on the screen, the exact coordinates of the places can be obtained only from the numerical calculation of nonlinear beam diffraction with allowance for the Kerr self-focusing.

The distance, at which the next filaments are formed, is illustrated by Fig. 3. On the map with the coordinates "moving" time t/τ_0 – distance from the screen z ," hot spots are plotted in the central layer of the pulse $t = 0$ and in the time layers shifted toward the leading edge by the interval t/τ_0 . These spots are connected by line segments, which allow us to see the filament history as a continuous chain of hot spots formed at successive moments in time in the case of a sufficiently short time step. In Fig. 3, the hot spots are enumerated in the order of their appearance in the central time layer ($t = 0$), which coincides with abscissa. The hot spots in the time layers shifted from the central one toward the leading edge of the pulse lie at the corresponding straight lines parallel to the abscissa.

Certainly, the filaments are formed nearest to the screen in the central layer of the pulse, because the power is the highest here. The power at the pulse edge is lower, and the nonlinear focus belonging to the same filament is formed farther from the screen. Therefore, the curves of the spatiotemporal trace of the filament are deflected to the right. The pulse layers following the central one are not considered, since they are subject to strong defocusing in the laser plasma, which is not included into the numerical model being used here.

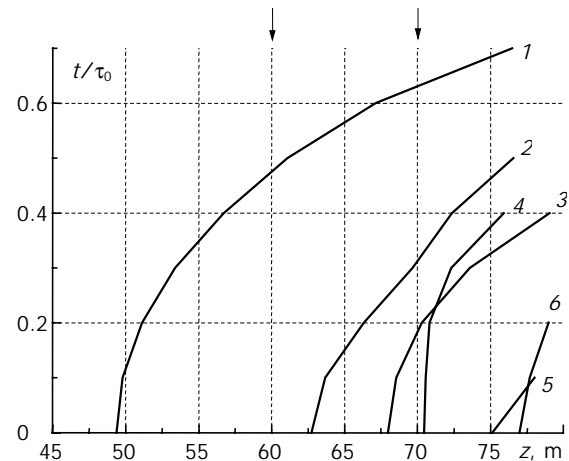


Fig. 3. Spatiotemporal cross sections of hot spots formed at the distance z from the screen at different moments of the "moving" time t for the Gaussian pulse (with the peak power $P_0 = 2 \cdot 10^{11}$ W and the cross section radius $a_0 = 0.92$ cm) scattered at the phase screen with the parameters $C_n^2 = 1.5 \cdot 10^{-14}$ cm $^{-2/3}$, $L_0 = 1$ m, $l_0 = 1$ mm, $\Delta z = 10$ m. The curve numbers correspond to the number of filaments in the central layer of the pulse.

The results presented indicate that the first filament is formed behind the screen in the pulse with the chosen parameters at the distance about 49 m. No filaments are formed closer to the screen. An observer is located, for example, at the distance of 60 m, which is marked by an arrow in Fig. 3, sees, as before, only one filament, in which the hot spot is caused by nonlinear focusing in the time layer shifted forward by $0.45\tau_0$ about the central one. At the distance of 70 m, also marked by an arrow in Fig. 3, an observer already sees three filaments, which were formed by hot spots in different time layers of the pulse: in the layers shifted forward by $0.6\tau_0$, $0.3\tau_0$, and $0.2\tau_0$ about the central one.

Due to the stochastic character of the considered filamentation, we can see in Fig. 3 the intersection of the filament traces (for example, curves 3 and 4). The point of intersection means that at this distance two hot spots, representing two filaments, are formed simultaneously in the same time layer of the pulse. It can be seen that, with the increasing distance from the screen z , the order of formation of these filaments in time alternates.

Certainly, the considered screen is only one of possible realizations of the ensemble of random phase screens with given statistical properties. Similar pattern of spatiotemporal traces of filaments was obtained for other phase screens as well. To obtain the average characteristics of the pattern of multifilamentation, pass on to the statistical analysis of the problem by the Monte Carlo technique.

Multifilamentation of the pulse scattered by the phase screen

To obtain statistical characteristics of the process of multifilamentation, an ensemble of random phase

screens with the given statistical characteristics has been synthesized. We have considered the screens with the modified Karman spectrum and the following parameters: structure constant $C_n^2 = 1.5 \cdot 10^{-14} \text{ cm}^{-2/3}$, outer scale $L_0 = 1 \text{ m}$, inner scale $l_0 = 1 \text{ mm}$, thickness of the turbulent medium layer $\Delta z = 10 \text{ m}$. For each screen located in the beginning of the path, numerical simulation of the nonlinear diffraction of the beam was carried out and the coordinates x, y, z of the initial formation of a series of hot spots forming filament were determined. Averaging was performed over the ensemble of 100 realizations of multifilamentation of the pulse scattered at statistically independent screens. The whole path length was 80 m.

The mean values of the distance z_f , at which a filament is formed, depending on its number, are shown in Fig. 4a for three values of the real pulse power. This figure also shows the statistical struggling (rms deviation) of these values caused by the random nature of the phase perturbations on the screen.

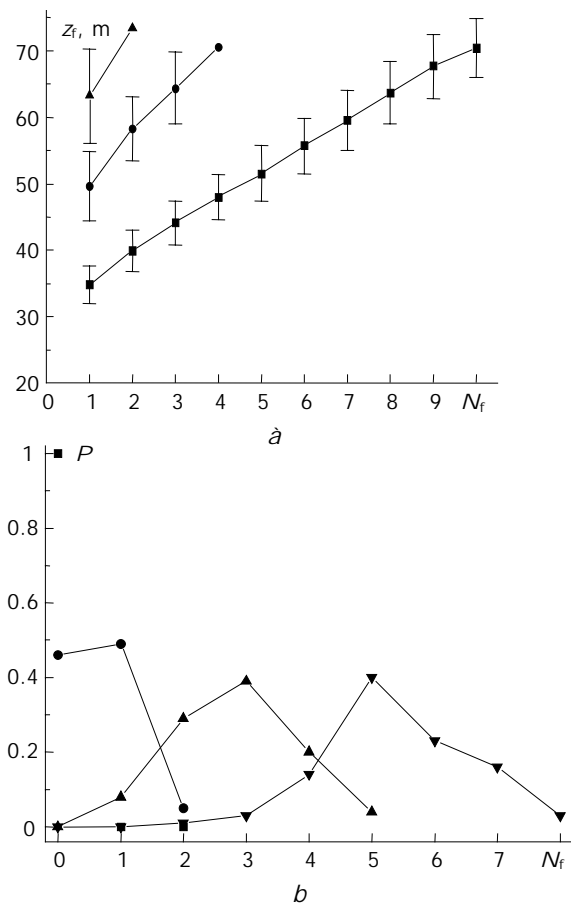


Fig. 4. Distance z_f to the beginning of formation of the N_f th filament at different peak pulse powers $P_0 = 1.0 \cdot 10^{11} \text{ W}$ (triangles), $1.3 \cdot 10^{11} \text{ W}$ (circles), $2 \cdot 10^{11} \text{ W}$ (squares) (a) and the probability P of observing the N_f filaments at the given distance $z = 25$ (squares), 35 (circles), 45 (triangle), and 55 m (inverted triangle) from the screen at $P_0 = 2 \cdot 10^{11} \text{ W}$ (b). Parameters of the phase screen are the same as in Fig. 3.

The number of filaments in the beam cross section increases with distance. As the peak power of the

pulse grows, filaments are formed closer to the phase screen, and their number at the given distance increases. Thus, as the peak power is doubled (from 10^{11} to $2 \cdot 10^{11} \text{ W}$), the mean distance to the first filament is almost halved, and the number of filaments observed at the distance $z = 65 \text{ m}$ increases from one to 7–9. In addition, the random deviation of the distance to the plane of filament formation in individual realizations from its average value decreases. Thus, with the increase of the peak power, we can predict the distance to the beginning of the next filament, in particular, to appearance of the first filament with high accuracy.

It can be seen from Fig. 4 that, because of the random scatter of the distances to the beginning of a filament, one, generally, cannot say with a high confidence how many filaments will be formed from pulse to pulse at the given distance from the screen. Figure 4b illustrates the probabilistic pattern of existence of a certain number of filaments at some distances z in the case of propagation of a pulse series. For convenience, the dots corresponding to the same distance are connected by straight-line segments. At the distance of 25 m (squares) no one filament will be certainly observed. At the distance of 35 m (circles), no filaments ($N_f = 0$) are formed only with the probability of 47%, and one filament ($N_f = 1$) will be observed with roughly the same probability. The probability to observe two and more filaments does not exceed 5%. As the distance z increases to 45 m (triangles), we will see three filaments with the probability of about 40%, two filaments with the probability of 30%, and four filaments with the probability of 20%. At the distance of 55 m (inverted triangles), most probable is observation of five filaments. Thus, the maximum of probability shifts toward the larger number of filaments with the increasing distance from the phase screen.

Filament bunch in the turbulent atmosphere

To analyze how the parameters of atmospheric turbulence affect the statistical characteristics of the filament bunch, a series of numerical experiments on the propagation of a collimated Gaussian beam along the atmospheric path has been conducted. The random fluctuations of the refractive index at the path were represented by a series of phase screens. The 80-m long path was divided into layers, each 10 m long. The turbulent phase change at each layer was simulated by a phase screen. It should be noted that the layers at the initial part of the path, adjacent to the exit aperture of the laser system, most strongly affect the characteristics of filaments. The analysis was carried out over the ensemble of 100 pulses, each propagating through statistically independent series of statistically independent phase screens.

Figure 5a shows the mean distances, at which the sequent filament is formed in the turbulent atmosphere. Qualitatively, the curves copy similar

dependences for the case of a single screen (see Fig. 4a). It should only be noted that the vertical bars on the lower curve show the 0.3-level confidence intervals for the mean value, rather than the statistical scatter of the filament coordinate. The obtained increase in the number of filaments with the increasing distance agrees with the experimental data.⁵

It is clearly seen that with the increase of the turbulence intensity (increase of the structure constant C_n^2), filaments are formed closer to the beginning of the path. Thus, as C_n^2 increases five times, the formation of several first filaments occurs, on the average, 5 m closer to the exit aperture of the beam (cf. circles and squares). The increase of the inner scale of turbulence l_0 , to the contrary, slows down the process of filament formation, though only a little (squares and triangles). The latter can be easily explained from the physical point of view. The large value of the inner scale corresponds to suppression of small-scale phase fluctuations, which just contain the power on the order of the critical one near the beam axis. Since the amplitude of fluctuations containing the critical power decreases, formation of hot spots occurs more slowly.

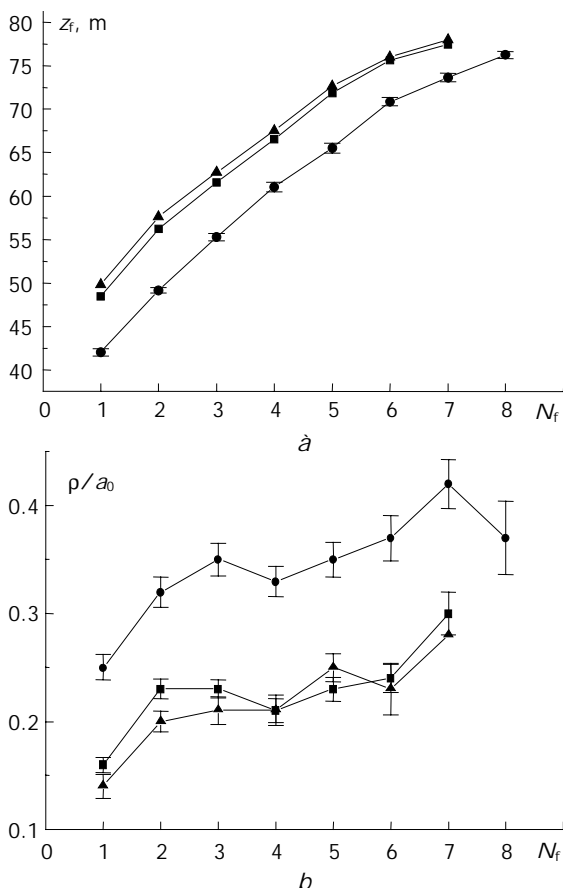


Fig. 5. Distance z_f to the beginning of filament formation (a) and the average size ρ of filament bunch (b) in the atmosphere with different parameters of turbulence: $C_n^2 = 1.5 \cdot 10^{-14} \text{ cm}^{-2/3}$, $l_0 = 1 \text{ mm}$ (circles); $C_n^2 = 3 \cdot 10^{-15} \text{ cm}^{-2/3}$, $l_0 = 1 \text{ mm}$ (squares); $C_n^2 = 3 \cdot 10^{-15} \text{ cm}^{-2/3}$, $l_0 = 5 \text{ mm}$ (triangles) in the case of propagation of the pulse with the peak power $P_0 = 1.2 \cdot 10^{11} \text{ W}$ and $a_0 = 0.82 \text{ cm}$.

Figure 5b illustrates the position of filaments in the cross section of the laser pulse. This figure shows the average values of confidence intervals for the shift of the sequent filament from the pulse axis. It can be seen that the first filament is formed, on the average, closest to the beam axis, where the intensity is higher.

With the increase of the filament number, we can see the tendency towards its deflection from the beam axis. As the turbulence intensity increases, the probability of appearance of filaments at the periphery of the cross section (circles) increases as well. In particular, the first filament is formed, on the average, at the longer distance from the axis. When C_n^2 increases fivefold, the mean deviation of the first filament from the laser beam axis almost doubles under the conditions considered. The next filaments also begin to form farther from the axis, which corresponds to the increase of the transverse dimension of the area in the cross section plane, where filaments are located.

Thus, with the increasing intensity of atmospheric turbulence, the bunch of stochastic filaments becomes wider. The effect of the inner scale on the widening of the filament bunch, as well as on the distance to the area of filamentation, is not too strong, though we can see the tendency to formation of the narrower filament bunch with the increase of l_0 .

Conclusions

1. The stochastic analysis of successive formation of filaments in the pulse scattered by a single phase screen has shown that the number of filaments increases with distance. Continuous series of hot spots in the cross section planes, forming a filament, arise in the central layer of the pulse and shift, as the beam propagates, into the time layers in the leading edge of the pulse. Experimentally observed localization of energy in several filaments is a consequence of sequential formation (with distance) of intensity maxima in the continuous chain of time layers of the pulse. Due to the stochastic nature of multifilamentation, the appearance of two or more hot spots at the same distance is possible in the same time layer.

2. The calculated probability density function of the number of filaments allows estimating the most probable number of filaments at the given distance from the exit aperture in a field experiment, as well as the average number of filaments and the standard deviation.

3. A bunch of randomly formed filaments is generated in the turbulent atmosphere. With the increasing distance the average number of filaments in the bunch and its transverse dimension increase. If the structure constant of atmospheric turbulence increases, the filament bunch is formed earlier, and it turns to be wider at the given distance. The inner scale of atmospheric turbulence influences weakly the statistical characteristics of the filament bunch, and with the growth of this parameter the distance to the beginning of the bunch increases a little and the bunch becomes narrower.

Acknowledgments

This work was supported, in part, by the Russian Foundation for Basic Research (grant No. 03-02-16939), European Office of the US Army Research (contract No. 62558-03-1 0029), and CRDF GAP (grant No. RPO-1390-TO-03).

References

1. S.A. Shlenov and V.P. Kandidov, *Atmos. Oceanic Opt.* **17**, No. 8, 565-570 (2004).
2. J. Kasparian, M. Rodriguez, G. Mejean, J. Yu, E. Salmon, H. Wille, R. Bourayou, S. Frey, Y.-B. Andre, A. Mysyrowicz, R. Sauerbrey, J.-P. Wolf, and L. Woste, *Science* **301**, No. 5629, 61-64 (2003).
3. K.Yu. Andrianov, V.P. Kandidov, O.G. Kosareva, S.L. Chin, A. Talebpour, S. Petit, W. Liu, A. Iwasaki, and M.-C. Nadeau, *Izv. Ros. Akad. Nauk, Ser. Fiz.* **66**, No. 8, 1091-1102 (2002).
4. S.L. Chin, A. Talebpour, J. Yang, S. Petit, V.P. Kandidov, O.G. Kosareva, and M.P. Tamarov, *Appl. Phys. B* **74**, 67-76 (2002).
5. W. Liu, S.A. Hosseini, B. Ferland, S.L. Chin, O.G. Kosareva, N.A. Panov, and V.P. Kandidov, *New J. Phys.* **6**, No. 6, 1-22 (2004).